Heliyon 5 (2019) e02555

Contents lists available at ScienceDirect

Heliyon

journal homepage: www.heliyon.com

Heliyon

Research article

An interdisciplinary approach to assess human health risk in an urban environment: A case study in temperate Argentina

Natalia Soledad Morandeira [a,*], Paula Soledad Castesana [a,b], María Victoria Cardo [a], Vanesa Natalia Salomone [a], María Victoria Vadell [a,1], Alejandra Rubio [a]

[a] Instituto de Investigación e Ingeniería Ambiental, UNSAM, CONICET, 3iA, Campus Miguelete, 25 de mayo and Francia, 1650, General San Martín, Provincia de Buenos Aires, Argentina

[b] Facultad Regional Buenos Aires, Universidad Tecnológica Nacional (UTN), Medrano 951, 1179, Ciudad Autónoma de Buenos Aires, Argentina

ARTICLE INFO

Keywords:
Ecological health
Applied ecology
Environmental hazard
Environmental risk assessment
Geography
Quality of life
Environmental pollutants
Geographic information system
Human health hazards
Risk assessment
Urban landscape
Zoonoses

ABSTRACT

Unplanned urbanization increases the exposure of people to environmental hazards. Within a landscape ecology framework, this study is a diagnosis of human health risk in San Martín, an urban district of Buenos Aires, Argentina. Risk was estimated by combining four hazard indexes (water and air pollution, and mosquito and rodent infestation) and a vulnerability index. Each index was obtained by integrating environmental and socio-demographic layers in a Geographic Information System. Spatial autocorrelation was assessed for each hazard, vulnerability and risk indexes using Moran's tests. Also, spatial associations between pairs of variables were addressed by means of Geographically Weighted Regressions. The robustness of hazard and vulnerability indexes was checked by a sensitivity analysis. In General San Martín district, 83.3% of the population is exposed to relatively high levels of at least one hazard; 7.4% is exposed to relatively high levels of all hazards (11.5% of the total area) and only 16.7% lives in areas of relatively low levels of all hazards (15.4% of the total area). Areas where hazard intensity was relatively high corresponded to those areas where the most vulnerable population lives, enhancing human health risk. The models for hazards and vulnerability were reasonably robust to changes in the weights of the variables considered. Our results highlight the spatially heterogeneous nature of human health risk in an urban landscape, and reveal the location of critical risk hotspots where reduction or mitigation actions should be focused.

1. Introduction

Although cities occupy only 5% of the Earth's terrestrial surface, they are home to more than half the global human population, and this percentage is likely to grow up to 60–92% by the end of the 21st century (Jiang and O'Neill, 2017). Unplanned urbanization is usually associated with environmental problems, including pollution, overcrowding, poor sanitation, inadequate waste disposal, exposure to etiologic agents of infectious diseases and insufficient access to safe drinking water (Moore et al., 2003). Human health risks are driven by the combination of environmental hazards and socio-demographic factors that determine which populations are more vulnerable to them (Lindley et al., 2006). Vulnerability depends on the extent to which health is sensitive to be affected by the environmental hazards, the magnitude of the exposure and the capacity to reduce the burden of a specific adverse health outcome ('biophysical vulnerability', *sensu* Brooks (2003)).

Among environmental hazards, pollution and zoonoses have been highlighted as the most important in urban areas (McGranahan et al., 2001). Urban air pollution represents a major environmental hazard to human health, particularly with respect to respiratory and cardiovascular affections, and cancer (World Health Organization, 2016). In developing countries, an estimated 42% of such diseases are linked to solid fuel smoke, vehicular and industrial emissions, and passive exposure to tobacco smoke (Maiztegui and Delucchi, 2010). A recognized group of air pollutants is volatile organic compounds (VOCs). Main urban sources of outdoor VOCs emissions are vehicular traffic, industries, dumps and landfills, while significant indoor sources include building and furnishing materials, and paints (Majumdar et al., 2014; Paciência et al., 2016). VOCs also play an important role in atmospheric chemistry as precursors of other secondary pollutants (Hubbell et al., 2005). Aromatic VOCs have

* Corresponding author.
E-mail address: nmorandeira@unsam.edu.ar (N.S. Morandeira).
[1] Present address: Instituto Nacional de Medicina Tropical (INMeT-ANLIS-MSAL), Misiones, Argentina.

https://doi.org/10.1016/j.heliyon.2019.e02555
Received 10 April 2019; Received in revised form 18 July 2019; Accepted 27 September 2019

proven diverse adverse health effects on humans. Benzene, for example, has been classified as a grade 1carcinogen (IARC Working Group, 2018).

Access to safe drinking water is essential for public health risk management (Hrudey et al., 2006). Lack of appropriate urban planning forces people to conduct individual perforations to the aquifer, to get direct intakes from watercourses, or to access an official water net with precarious connections (Moore et al., 2003). These alternative water sources may be contaminated by inadequately disposed liquid effluents and uncontrolled garbage disposal (Cabral, 2010). Over 700 organic and inorganic pollutants have been reported in water bodies, many of which are dangerous given their toxicity and potential carcinogenesis (Brito et al., 2015). The most common water-related diseases include diarrhea, cholera, infectious hepatitis and arsenicosis (World Health Organization, 2011).

Zoonoses are diseases transmitted to humans either by direct contact with infected secretions of animal hosts, or mediated by vectors. The occurrence and distribution of zoonotic diseases are driven by complex dynamics of environmental, ecological and social factors (World Health Organization, 2014). In urban areas, rodents are the main vertebrate pests (Singleton et al., 2003), often acting as reservoirs or carriers of leptospirosis, salmonellosis, plague, rat-bite fever, and hantavirus renal and pulmonary syndromes (Himsworth et al., 2013; Meerburg et al., 2009). Likewise, in urban settings, anthropophilic mosquitoes such as *Aedes aegypti* and *Culex* spp. breed mainly in man-made containers and are the main vectors of dengue, chikungunya, Zika, West Nile fever and St. Louis encephalitis (Weaver et al., 2018).

Landscape ecology provides a conceptual framework to integrate multiple hazards and vulnerability by addressing their inherent spatial complexity, thus obtaining risk maps with a quantitative approach. Risk assessment can be substantially improved by the inclusion of spatial analyses of the data in a Geographic Information System (GIS) (Di Salvo et al., 2018; Liu et al., 2019; Poggio and Vrščaj, 2009), which also represents an advantage to communicate results, discuss the social perception of environmental hazards and plan management actions (Lahr and Kooistra, 2010; vonHedemann et al., 2015).

Multi-hazard risk assessments that include vulnerability estimations have been applied worldwide at a district or a landscape scale for multiple purposes, *e.g.*, flood risk in urban areas (Kaźmierczak and Cavan, 2011; Kubal et al., 2009); environmental risks of deltaic socio-ecological systems (Hagenlocher et al., 2018); impact of catastrophic events (Marzocchi et al., 2012); climate change-related risk (Lindley et al., 2006). In Argentina, childhood health risk associated with sanitation and agro-industrial activities has been studied at the country level (Maiztegui and Delucchi, 2010).

Using a landscape ecology framework and aided by GIS tools, the aim of this study was to make a diagnosis of human health risk in a temperate urban area, and to analyze its spatial pattern at a district scale. We quantified and mapped human health risk by integrating hazards and vulnerability in a case study, the district General San Martín (Buenos Aires, Argentina), a residential and industrial urban area that is part of the greatest megalopolis of temperate South America. The methodological approach and conceptual framework integrate theories and tools from urban and landscape ecology, geospatial data, spatial statistics and GIS approaches.

This article is organized as follows: we first describe the study area and the minimal sampling units, and summarize our conceptual framework. Next, we develop the hazard indexes and maps (water pollution, air pollution, mosquito infestation and rodent infestation hazards), and the vulnerability index and map, referring to the source variables and their management in a GIS environment. We obtained hazard intensity and also combinations of relatively low or high hazard levels to summarize the four sources of environmental hazards. Also, we combined hazards and vulnerability to obtain a risk intensity map. We performed the following analyses on these products: spatial heterogeneity, spatial relations between pairs of index values and sensitivity to check robustness. Results are presented aided by maps and discussed within an urban ecology framework.

2. Methods

2.1. Study area

General San Martín district is located in Buenos Aires Province, Argentina (central coordinates: 34°34′S 58°33′W, Fig. 1). It covers 56.3 km^2, with 414,196 inhabitants and 7,356 inhabitants/km^2 (Instituto Nacional de Estadística y Censos, 2010). Climate is temperate humid. The district includes residential, commercial and industrial neighborhoods. Industries in the district are mainly metallurgical, chemical, petrochemical, and textile. As only urban areas were considered in this study, the area comprised between Camino del Buen Ayre highway and Reconquista River (Fig. 1) was excluded from the analysis (total study area 50.2 km^2). Potential hazard sources located within a buffer of 1 km around the limits of the study area were included in the analysis. In this work, straight-line buffers were used.

2.2. Minimal sampling units

To produce hazard, vulnerability and risk maps, several spatial layers were gathered from available sources, recombined or generated *ad hoc* (Table 1). As these were vector or raster layers at different spatial resolutions, to combine them we defined the minimal sampling units as the census tracts of the last "Population, Households, and Housing National Census", abbreviated INC from now on (Instituto Nacional de Estadística y Censos, 2010) (Fig. 1(c)). The census tract is the minimum resolution used by the INC and consists of a polygon covering several blocks, comprising *ca.* 300 dwellings. A total of 434 census tracts covered the study area, each track containing between 20 and 681 dwellings (each dwelling has one or more households) and covering between 0.01 km^2 and 1.91 km^2. Geographic data was restructured and summarized in the attribute table of the census tract layer (a polygon vector layer): *e.g.*, the raster altitude layer was converted to a vector layer with mean altitude per census tract.

2.3. Conceptual framework

The conceptual framework of human health risk assessment in the study area is summarized in Fig. 2, and involves product maps for each hazard (water and air pollution, and mosquito and rodent infestation), for vulnerability, and for risk. In general terms, we considered that human health risks are driven by hazards and vulnerability, following Lindley et al. (2006). For each hazard and vulnerability index, we constructed an equation that included multiple variables. Variables used to compute hazard and vulnerability indexes were either additive *primary factors* with constant weights to relativize its contribution respect to other primary factors; or multiplicative *secondary factors* applied to the primary factors. Secondary factors are considered as potential enhancers to the hazard: *e.g.*, a weighting factor of 1.5 assumes that the hazard resulting from the primary factors (scaled between 0 and 1) can be increased by 50% by the worst value of the secondary factor. Intermediate calculations, as well as the final indexes, were scaled between 0 and 1 (minimum and maximum hazard/vulnerability/risk, respectively). Thus, resulting products have no absolute values and should be interpreted as relative indexes with extent on the study area.

The notation used for equations was: capital letters indicate whether the index refers to a hazard (W = water, A = air, M = mosquitoes, R = rodents), vulnerability (V) or risk (R); subscript i indicates that the index is computed per census tract i ($1 \leq i \leq 434$); subscript p indicates that the variable is a primary factor, subscript s indicates that the variable is a secondary factor; and the subscripts j ($j \geq 1$) were used to enumerate primary or secondary factors. In each equation, subscripts indicate the minimum and maximum values used to scale the index (*e.g.*, 0–1 for a primary factor; 1–1.5 for a secondary factor).

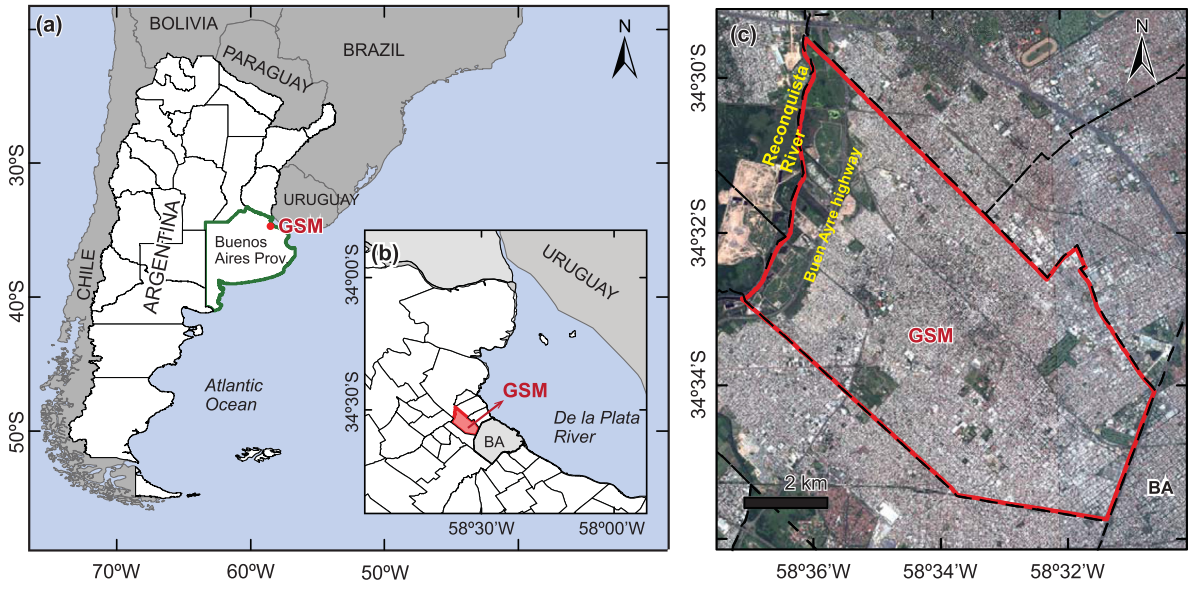

Fig. 1. Study area. The case study was General San Martín (GSM), in Buenos Aires Province, Argentina. (a) Location in Argentina. (b) Location in Buenos Aires Province. Note that the study area is neighbor to the capital city of Argentina, Buenos Aires City (BA). (c) General San Martín and neighbor districts. An optical satellite image is shown (WorldView-3, acquired on November 15th 2014, color composition: Red = band no. 5 (630–690 nm); Green = band no. 3 (510–580 nm); Blue = band no. 2 (450–510 nm). Satellite image courtesy of the DigitalGlobe Foundation. For a detail of limits of the census tracts –i.e., the minimal sampling units– see Figs. 2, 3, 4, 5, and 6. See electronic version for color images.

Table 1

Geographic variables used in the hazard and vulnerability indexes. Input sources are detailed along with the original spatial resolution of the variable: demographic information per census tracts, derived from the last national population census of the INC (Instituto Nacional de Estadística y Censos, 2010); point vector data provided by SIT-UNSAM (Extension Secretary of San Martín University) and National Secretary of Energy; industry records from OPDS (Provincial Organism for Sustainable Development); raster product SRTM (Shuttle Radar Topography Mission); WorldView-3 satellite imagery; and self-generated products. Columns refer to: Water pollution hazard (W), Air pollution hazard (A), Mosquito infestation hazard (M), Rodent infestation hazard (R) or Vulnerability (V). The hazard and vulnerability indexes for which these geographic variables were used are mentioned following the scientific notation used along the text, with the first letter indicating the hazard or vulnerability and the second letter indicating a primary (*p*) or secondary (*s*) factor. Parenthesis point out that the variable was used as an intermediate input for computing hazard indexes.

Variable	Sources of the geographical inputs	Spatial representation	W	A	M	R	V
Percentage of households without connection to a potable water public network	INC	Census tracts	W_p				
Source of water used for human consumption	INC	Census tracts	W_{s1}				
Percentage of households without a sewer connection	INC	Census tracts	W_{s2}		M_{p4}	R_{p7}	
Proximity to industries weighted by their environmental complexity level	SIT-UNSAM, OPDS	Point data	W_{s3}	A_{p4}			
Proximity to dumps and landfills	Photointerpretation of WorldView-3 imagery and ancillary literature	Polygons digitalized on 0.31 m pansharpened scenes	W_{s4}	A_{p3}			
Proximity to cemeteries, dumps and open landfills	Photointerpretation of WorldView-3 imagery	Polygons digitalized on 0.31 m pansharpened scenes			M_{p1}	R_{p3}	
Low topography	SRTM	30 m raster grid	W_{s5}	A_{s1}	M_{p6}		
Proximity to gas stations	National Secretary of Energy	Point data		A_{p1}			
Vehicular and train emissions	Self-generated based on public transport circulation and traffic records	Line data		A_{p2}			
Vegetated/Non-vegetated surfaces	NDVI threshold on WorldView-3 imagery	1.24 m raster grid		A_{s2}	(M_{p3})	R_{p1}	
Water storage at the dwelling	Self-generated based on INC data	Census tracts			M_{p2}		
Proximity to open canals and streams	Photointerpretation of WorldView-3 imagery	Lines digitalized on 0.31 m pansharpened scenes			M_{p5}		
Water availability	Self-generated based on "Water storage at the dwelling" and "Proximity to open canals and streams"	Census tracts and 0.31 m pansharpened scenes				R_{p5}	
Poor quality of construction materials of the dwellings	INC	Census tracts				R_{p2}	V_{p56}
Human population density	INC	Census tracts			(M_{p3})	R_{p4}	
Proximity to food industries weighted by their environmental complexity level	SIT-UNSAM, OPDS	Point data				R_{p6}	
Proportion of children and elderly population	INC	Census tract					V_{p1}
Overcrowding	INC	Census tract					V_{p2}
Illiteracy rate	INC	Census tract					V_{p3}
Economic inactivity rate	INC	Census tract					V_{p4}
Distance to primary health centers	SIT-UNSAM	Point data					V_{p6}

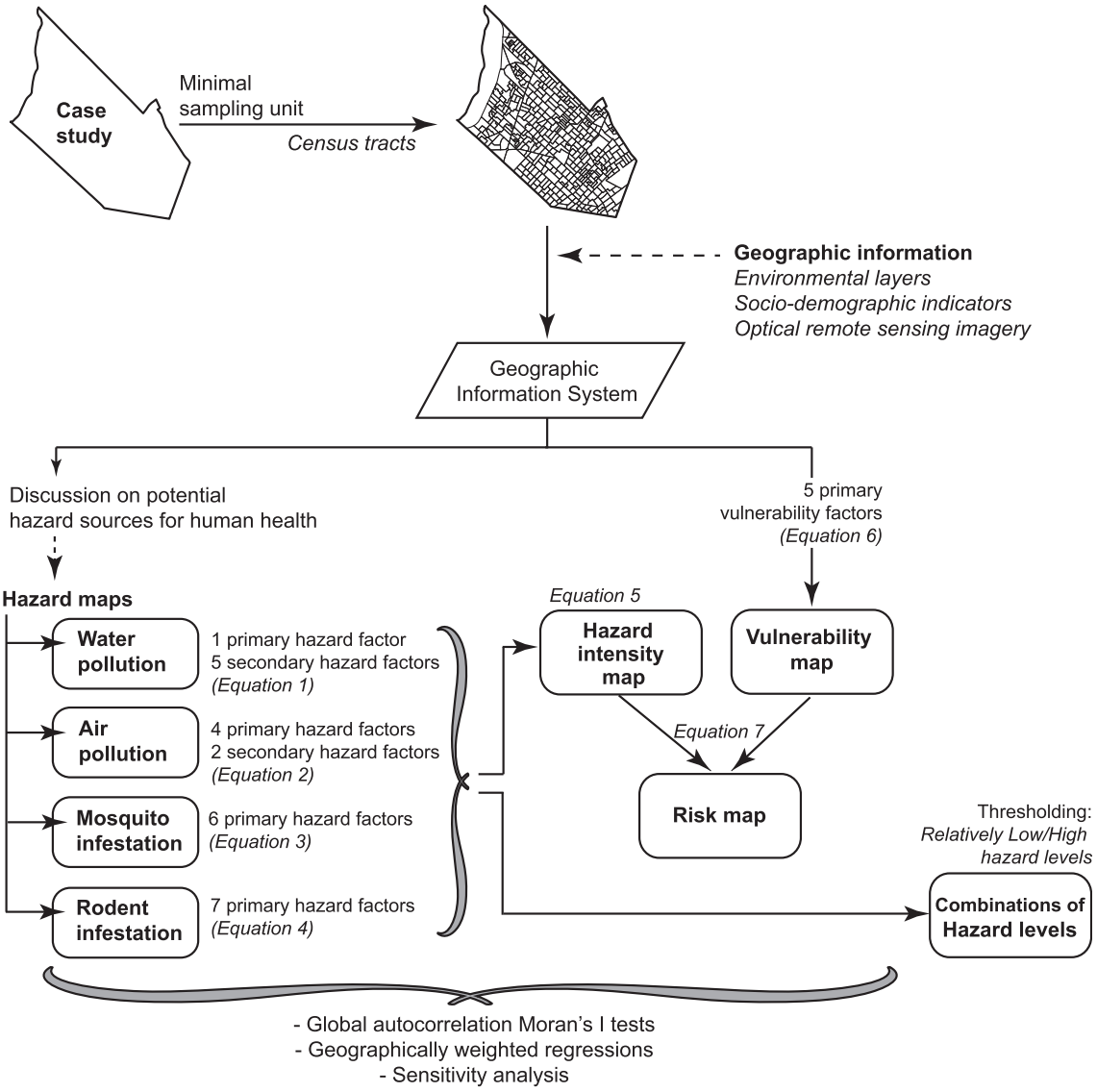

Fig. 2. Methodological scheme. Environmental layers, socio-demographic indicators and remote sensing imagery were integrated in a GIS. Hazard, vulnerability and risk indexes were obtained and mapped for the study area (General San Martín, abbreviated GSM), with census tract as the minimal sampling unit. Product maps are pointed out with a rounded rectangle. See text for details on the procedures, variables and equations.

2.4. Hazard maps

2.4.1. Water pollution hazard

The absence of connection to a safe water public network (variable "Percentage of households without piped connection to a water public network per census tract *i*", W_{pi}) was considered as the primary factor affecting drinking water quality. Provided the household was not connected to the network, several secondary factors (W_{sji}) were considered to have an extra negative impact on water quality. The index W_i of water pollution hazard per census tract *i* was obtained by applying Eq. (1):

$$W_i = \left[W_{pi} \cdot (W_{s1i} \cdot W_{s2i} \cdot W_{s3i} \cdot W_{s4i} \cdot W_{s5i})\right]_{0-1} \quad (1)$$

Secondary factors W_{sj} were:

W_{s1}. Source of drinking water. Households without connection to the public water network may obtain drinking water from water cisterns or deep wells (low relative hazard), river water, rainwater or shallow wells (high hazard). The extended formula to compute the weights for W_{s1} was: $W_{s1i} = [1 \cdot (\%$ of households in census tract *i* using water cisterns or deep wells$) + 2 \cdot (\%$ using riverwater, rainwater or shallow wells$)]_{1-1.50}$.

W_{s2}. Percentage of households without a sewer connection. Households without a sewer connection may experience contamination of the shallow aquifers used for water uptake. Types of on-site sanitation were: cesspits with a septic chamber (low hazard), cesspits with no septic chamber (medium hazard), rudimentary pits (high hazard). The extended formula to compute the weights for W_{s2} was: $W_{s2i} = [1 \cdot (\%$ of households in census tract *i* using cesspits with septic chambers$) + 2 \cdot (\%$ using cesspits without septic chambers$) + 3 \cdot (\%$ using rudimentary pits$)]_{1-1.50}$.

W_{s3}. Proximity to industries weighted by their environmental complexity level. Groundwater can be contaminated with industrial effluents and waste. A georeferenced list of 871 industries within the study area was provided by the Extension Secretary of San Martín University (SIT-UNSAM). Besides, a non-georeferenced database of industries with their environmental complexity levels (ECL) comprising 4,764 records was available from the Provincial Organism for Sustainable Development (OPDS; updated to 2015). OPDS groups industries into 1st, 2nd and 3rd category (with increasing environmental complexity) according to industry type, effluents and waste, potential risks to the population or environment, dimensions, and location. Matching these two databases by

postal address, industry name and/or name of the owner resulted in 559 georeferenced industries with ECL categorization (64% of the SIT-UNSAM database) and 312 non categorized georeferenced industries.

We constructed buffers of 100 m around each of the 871 georeferenced industries and computed the percentage of each census tract area that fell within the buffers, discriminating by ECL categories when available. The extended formula to compute the weights for W_{s3} was: W_{s3i} = [3 • (% of census tract *i* close to 3rd category industries) + 2 • (% of census tract *i* close to 2nd category industries) + 1 • (% of census tract *i* close to 1st category industries or non-categorized industries)] $_{1–1.25}$.

W_{s4}. Proximity to dumps and landfills. Groundwater can be affected by pollutants leaching from solid waste. Dumps and landfills were digitalized by photointerpretation of a cloud-free WorldView-3 scene acquired on November 14th 2015 (imagery courtesy of Digital Globe Foundation) with a high spatial resolution (pixel size: 1.24 m for multispectral bands and 0.31 m for the panchromatic band). The scene was corrected to top-of-atmosphere reflectance. A pansharpening procedure was conducted to achieve a resolution of 0.31 m for multispectral pansharpened bands. Digitalization was conducted at a 1:2,000 scale and ancillary information were used to aid photointerpretation (Igarzabal de Nistal et al., 2012; Miño, 2012). Polygons were labeled as: relatively high hazard, considered to impact within a 400 m buffer area (based on Igarzabal de Nistal et al. (2012) and similar to distances reported by Taylor and Allen (2006)); and relatively low hazard, considered to impact within a 100 m buffer area. High hazard was assigned to consolidated open dumps (open dumps with an area over 1 ha or open dumps inside landfills with a volume higher than 500 m^3) and junk car dumps. Low hazard was assigned to closed landfill areas and small non-consolidated open dumps. The extended formula to compute the weights for W_{s4} was: W_{s4i} = [% of census tract *i* within a 100 m buffer area to low hazard dumps and landfills or within a 400 m hazard area to high hazard dumps and landfills] $_{1–1.25}$.

W_{s5}. Low topography. Low topography was considered a proxy for eventual floods associated with heavy rain, which have a negative impact on groundwater quality by facilitating the horizontal transference of pollutants from cesspits, ditches or dumps. The digital elevation model of the Shuttle Radar Topography Mission (SRTM) was used (raster layer with a spatial resolution of 30 m). The weight for W_{s5} was computed as: W_{s5i} = [maximum SRTM altitude for the study area – mean SRTM altitude in census tract *i*] $_{1–1.10}$.

2.4.2. Air pollution hazard

To become independent from household practices, only outdoor anthropic sources of VOCs were considered, focusing on BTEX chemicals (benzene, toluene, ethylbenzene and xylene) due to their adverse health effects and the existence of potential sources in the study area. We considered four variables indicating the proximity to main anthropic sources of BTEX as primary factors, along with two secondary factors. The index A_i of air pollution hazard per census tract *i* was obtained by applying Eq. (2):

$$A_i = \left[\left(3 \cdot A_{p1i} + 3 \cdot A_{p2i} + 2.5 \cdot A_{p3i} + 2 \cdot A_{p4i}\right)_{0-1} \cdot \left(A_{s1i} \cdot A_{s2i}\right)\right]_{0-1} \quad (2)$$

Primary factors A_{pj} were:

A_{p1}. Proximity to gas stations. We computed buffer distances to a point vector layer of gas stations provided by the National Secretary of Energy (Table 1). High hazard and low hazard were set at distances lower than 100 m, and between 100 and 200 m, respectively (Correa et al., 2012). The extended formula to compute the weights for A_{p1} was: A_{p1i} = [0.6 • (% of census tract *i* within a 100 m buffer area to gas stations] + 0.4 • (% of census tract *i* between 101 and 200 m to gas stations)] $_{0–1}$.

A_{p2}. Proximity to vehicular traffic and non-electric train rails. Data on annual average daily traffic (AADT) were only available for a national highway (General Paz Avenue, AADT: ~209,000 vehicles in 2016, source: National Road Direction). In addition, we assumed as high traffic roads all other roads with public transport (bus) circulation, and gathered (and digitalized) the information on bus routes. Roads with public transport circulation indicate high levels of human activity, and are also associated with high traffic from particular cars and trucks. Train railroads used by diesel engine formations were also considered. The extended formula to compute the weights for Ap_2 was: Ap_{2i} = [(% of census tract *i* within a 200 m buffer area to the national highway) + [(% of census tract *i* within a 100 m buffer area to high traffic roads or train rails)] $_{0–1}$.

A_{p3}. Proximity to dumps and landfills. Equivalent to W_{s4}, but scaled between 0 and 1.

A_{p4}. Proximity to industries weighted by their environmental complexity level. Certain types of industries present in the study area use solvents, lubricants, greases or waxes related to evaporative BTEX emissions: metal-mechanics, printing offices, leather shoe factory, coating application, among others. The number of locations where these activities are carried out per census tract is highly correlated to the total number of industries per census tract (r = 0.92). In order to consider these non-stack emissions, we constructed buffers of 100 m around industries discriminated by ECL categories, in a similar way to W_{s3}, but scaled between 0 and 1.

Secondary hazard factors A_{sj} were:

A_{s1}. Low topography. In low areas, limited atmospheric circulation can generate an accumulation of air pollutants. The index is equivalent to W_{s5}, but scaled between 1 and 1.20.

A_{s2}. Non-vegetated surfaces. As pollutants can be absorbed by vegetation, census tracts with high proportions of non-vegetated surfaces have a relatively higher air quality hazard. The high resolution WorldView-3 scene was processed to top of atmosphere reflectance and the Normalized Difference Vegetation Index (NDVI) was computed (Tucker, 1979), using bands 7 and 5 as Infrared and Red reflectance, respectively. An NDVI threshold was chosen by analyzing the NDVI histogram of the scene and using a Jenks' natural break criterion (Jenks and Coulson, 1963): pixels with NDVI <0.33 were assigned to non-vegetated surfaces. Non-vegetated areas were computed per census tract, and the percentage of non-vegetated surfaces per census tract *i* was computed and scaled between 1 and 1.20.

2.4.3. Mosquito infestation hazard

Six primary factors were considered as determinants of favorable conditions for mosquito proliferation in urban settings. The index M_i of mosquito infestation hazard per census tract *i* was obtained by applying Eq. (3):

$$M_i = \left[3 \cdot M_{p1i} + 3 \cdot M_{p2i} + 3 \cdot M_{p3i} + 2 \cdot M_{p4i} + 2 \cdot M_{p5i} + M_{p6i}\right]_{0-1} \quad (3)$$

Primary factors M_{pj} were:

M_{p1}. Proximity to cemeteries, dumps and open landfills. These sites are considered key sources of mosquitoes in urban and suburban settlements due to their high density of water-filled containers (Rubio et al., 2013). Typical flight range for container mosquitoes varies between 100 m (*Aedes aegypti*) and 1000 m (*Culex pipiens*) (Verdonschot and Besse-Lototskaya, 2014), and females are expected to stay near their larval habitat if their basic requirements (sugar substances, blood sources, shelter and water-field containers) are met (Vezzani, 2007). From the map of dumps and landfills computed for the factor W_{s4}, we excluded closed landfills and added the San Martín cemetery, digitalized by photointerpretation on the aforementioned WorldView-3 scene. The extended formula to compute the weights for M_{p1} was: M_{p1i} = [% of census tract *i* within a 100 m buffer area to dumps, open landfills or cemetery] $_{0–1}$.

M_{p2}. Water storage at the dwelling. Peridomiciliary water storage in containers is common in dwellings without connection to a water public network (Schmidt et al., 2011) and is also expected if the toilet lacks a push button. The extended formula to compute the weights for M_{p2} was: M_{p2i} = [(% of the households of census tract *i* without connection to public network nor dwells with motor water pumps) x (% of the

households without toilet with push button)] $_{0-1}$.

M_{p3}. Compromise between vegetated surfaces and human population density. Adult mosquitoes feed on nectar and plant juices, but females of most species need to obtain nutrients from a blood meal before they can produce eggs. Thus, resources for mosquitoes are enhanced when high vegetated surfaces converge with high population density (Rubio et al., 2013; Schmidt et al., 2011). We weighted green surface coverage estimated with the WorldView-3 NDVI criterion (see A_{s2}) with thresholds defined by Jenks' Natural Breaks: $k = 1$ for green areas <19.8% of the census tract; $k = 2$ for green areas between 19.8% - 33.7%; $k = 3$ for green areas >33.7%. Human population density was computed on a GIS by considering census tract areas. The extended formula to compute the weights for M_{p3} was: M_{p3i} = [Density of human population per census tract $i + k \cdot$ (% of green surfaces per census tract i)] $_{0-1}$.

M_{p4}. Percentage of households without a sewer connection. Except for *Ae. aegypti*, which breeds exclusively in container habitats, many urban mosquito species are favored by the occurrence of ponds and ditches (Irwin et al., 2008), which are usually formed and/or built in the soil to facilitate the drainage of domestic wastewater. This hazard factor is equivalent to W_{s2}, but scaled between 0 and 1.

M_{p5}. Proximity to open canals and streams. Open canals and stream margins, and in some cases the waste associated with them, provide a suitable habitat for mosquitoes. Canals and streams were digitalized on the pansharpened WordlView-3 scene. The percentage of the census tract within a buffer zone of 100 m to waterways was computed.

M_{p6}. Low topography. Low topography may favor stagnant water accumulation. Equivalent to W_{s5}, but scaled between 0 and 1.

2.4.4. Rodent infestation hazard

Rodent species that are hosts of several zoonoses in the area are *Rattus norvegicus, R. rattus, Mus musculus* and *Oligoryzomys flavescens* (Carvalho de Oliveira et al., 2014; Meerburg et al., 2009). The index R_i of rodent infestation hazard per census tract i was obtained by applying Eq. (4), which included seven primary hazard factors:

$$R_i = \left[3 \cdot R_{p1i} + 3 \cdot R_{p2i} + 2.5 \cdot R_{p3i} + 2.5 \cdot R_{p4i} + 2 \cdot R_{p5i} + 2 \cdot R_{p6i} + R_{p7i}\right]_{0-1} \quad (4)$$

Primary factors R_{pj} were:

R_{p1}. Presence of vegetated surfaces. Rats need vegetated or ground surfaces for shelter and burrow construction (Cavia et al., 2009; Feng and Himsworth, 2014). Vegetable food is also important for native rodent species and for *M. musculus* (Cavia et al., 2009; Masi et al., 2010). *R. norvegicus* needs soil to construct its burrows (Traweger et al., 2006), which in cities is usually available in parks, gardens, and unpaved roads. The presence of fruit trees favors *R. norvegicus* and *R. rattus* (Masi et al., 2010). Gardens and backyards are usually associated with pets (and pet food) and with unused objects that make good rodent shelters (Tamayo-Uria et al., 2014). The percentage of vegetated surface per census tract is the complement of A_{s2}, scaled between 0 and 1.

R_{p2}. Poor quality of building materials of the dwellings. Poor quality materials or poor quality constructions allow rodent entrance to the dwelling (Masi et al., 2010). This variable was available per census tract i (Table 1).

R_{p3}. Proximity to cemeteries, dumps and open landfills. These environments are usually vegetated, and provide food and shelter for rodents (Masi et al., 2010; Lambert et al., 2017). Equivalent to M_{p1}.

R_{p4}. Human population density. More human population density is positively associated with more garbage, particularly with food and organic waste, which provide food for rodens (Masi et al., 2010; Feng and Himsworth, 2014). This factor was computed as an intermediate step to obtain M_{p3}.

R_{p5}. Water availability. Rodents need water, particularly *R. norvegicus* (Cavia et al., 2009). To estimate water availability, we considered the probability of water storage at the dwelling (M_{p2}) and the proximity (<100 m) to open canals and streams (M_{p5}).

R_{p6}. Proximity to food industries weighted by their environmental complexity level. Sites close to food industries provide a good habitat for rodents because of the availability of food and organic waste (which constitutes the main food resource for rodents in urban habitats; Feng and Himsworth, 2014), especially for *R. rattus* that can adapt to low vegetated surfaces. This factor is analog to W_{s3}, but we only considered food industries. No 3rd category food industries were recorded.

R_{p7}. Percentage of households without a sewer connection. Households without a sewer connection and with rudimentary pits or cesspits may allow rodent entry (Feng and Himsworth, 2014). This hazard factor is equivalent to W_{s2}, but scaled between 0 and 1.

2.4.5. Hazard intensity and combinations of hazard levels

Two maps resulting from the combination of hazard indexes were obtained. Hazard intensity per census tract i was computed following:

$$H_i = \left[W_i + A_i + M_i + R_i\right]_{0-1} \quad (5)$$

Different combinations of hazard index values could result in the same hazard intensity value for a given census tract, *e.g.* a high hazard intensity could result equally from one very high and three low hazard indexes, or from four intermediate hazard indexes. Therefore, an index of hazard types was computed. Each hazard was categorized in relatively low and high levels by using a threshold defined through Jenks' Natural Breaks with *BAMMtools* (Rabosky et al., 2014) in R Project (R Core Team, 2015). Next, each census tract was assigned to one out of the 16 possible combinations resulting from the combination of relatively low and high hazard levels for each variable.

2.5. Vulnerability

We considered six primary factors that may contribute to vulnerability and assigned equal weights to each of them. The first five factors were directly obtained by census tract from INC (Table 1), i.e., they derive from demographic surveys averaged at the census tracts. All intermediate V_j indexes were scaled between 0 and 1, then vulnerability V_i was computed as:

$$V_i = \left[V_{p1i} + V_{p2i} + V_{p3i} + V_{p4i} + V_{p5i} + V_{p6i}\right]_{0-1} \quad (6)$$

V_{p1}. Proportion of children and elderly population. People younger than 14 years and older than 65 years are usually more vulnerable to diseases and spend more time in their dwellings.

V_{p2}. Overcrowding. Overcrowded housing promotes the spread of diseases such as measles, respiratory infections, diarrheal diseases and vector-borne diseases, many of them related to deficient sanitation.

V_{p3}. Illiteracy rate. Low levels of education create disadvantageous conditions to access or interpret information about surrounding health hazards and how to deal with them; and to access to well-paid jobs.

V_{p4}. Economic inactivity. A person without employment nor occupation suffers damage to their self-esteem and has limited access to medical coverage and other services. Nutritional and household deficiencies are also expected.

V_{p5}. Poor quality of construction materials of the dwellings. Dust, moisture, cold and injuries associated with low quality dwellings may affect human health. Equal to R_{p2}.

V_{p6}. Distance to primary health centers. Access to health care may decrease with increasing distance to health care facilities. This variable was generated by us, from a database of primary health centers: we computed the average distance of each census tract to the closest primary health center.

2.6. Human health risk

Human health risk was computed as:

$$R_i = \left[H_i \cdot (V_i + 1)\right]_{0-1} \quad (7)$$

Note that –prior to rescaling between 0 and 1– risk cannot equal 0 unless H_i is minimum and equals 0. This formula expresses that even with minimum V_i, a population exposed to high hazard levels could be under high sanitary risk.

2.7. Spatial patterns

Spatial heterogeneity of each hazard, vulnerability and risk indexes was first analyzed with Moran's *I* tests. This is a global test for spatial autocorrelation appropriate for areal data (Bivand et al., 2008), which compares the index value in each census tract with the value weighted by the contribution of neighbor census tracts. We considered that neighbor census tracts to a given census tract *i* were those sharing at least one vertex with *i* (Queen-style census tract contiguities). Equal spatial weights were assigned for the set of neighbors of each census tract *i*.

Next, to analyze the spatial relations between pairs of index values, geographically weighted regressions (GWR) were computed (Bivand et al., 2008): if the association was significant, varying slopes were obtained and plotted for all census tracts. Thus, not only the existence of a correlation between index values but also its magnitude over the study area was addressed. Libraries *spdep* (Bivand and Piras, 2015), *GWmodel* (Gollini et al., 2015) and *rgdal* (Bivand et al., 2018) in R Project were used.

2.8. Sensitivity analysis

In the construction of hazard and vulnerability indexes, the variables selected and the weight given to each were based on the existing literature, our expertise and perception of the local system. To test the robustness of each index and their derived maps, we conducted a

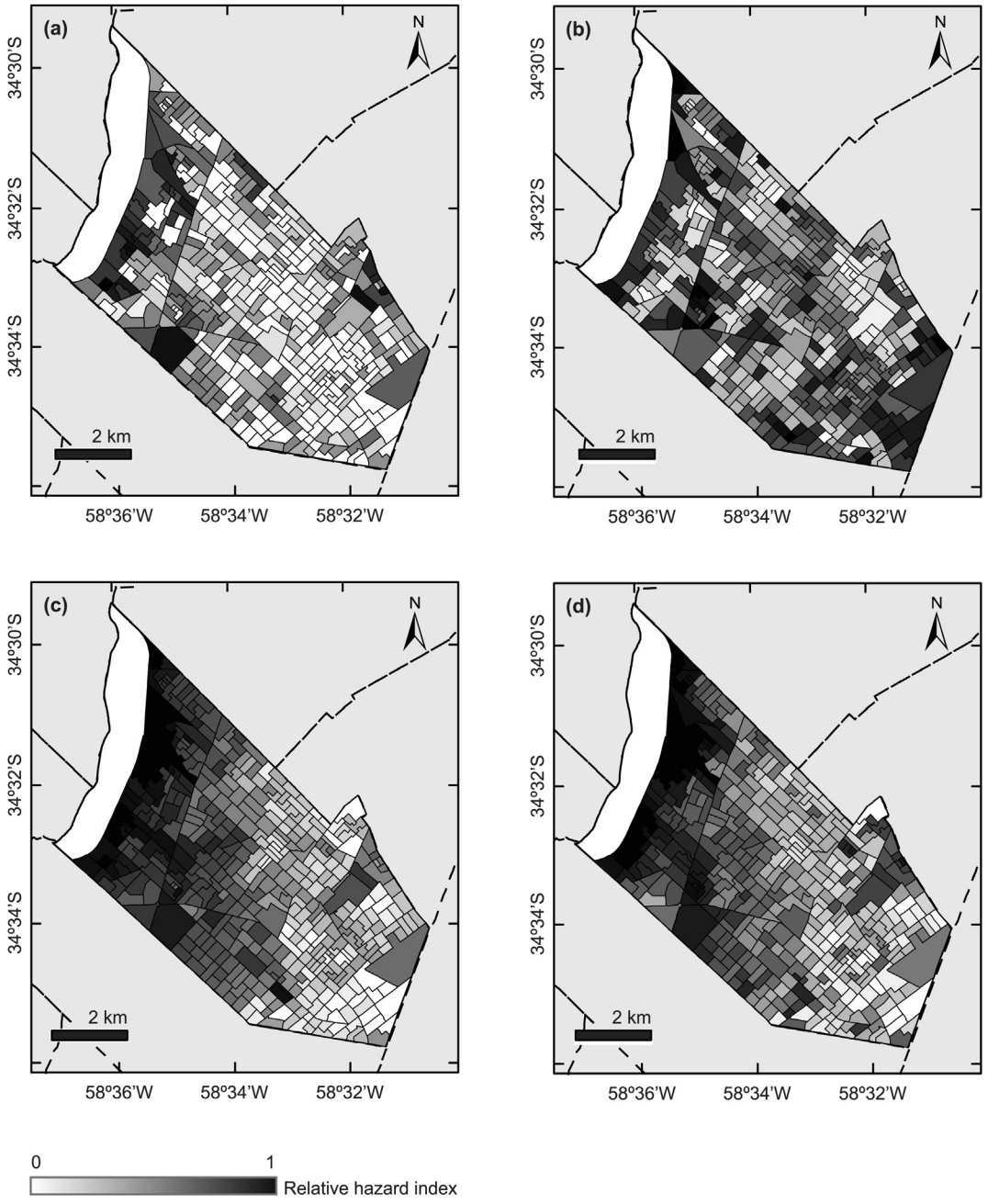

Fig. 3. Hazard maps. Relative hazard indexes, ranging between 0 and 1, per census tract. (a) Water pollution hazard. (b) Air pollution hazard. (c) Mosquito infestation hazard. (d) Rodent infestation hazard.

sensitivity analysis. The sensitivity of each primary or secondary factor is related to the amount of uncertainty in the estimation of hazard and vulnerability, and ultimately contributes to the uncertainty of the final risk model. In the hazard indexes, for each primary factor we considered the effect of varying the originally assigned weight by 10, 20 and 50% up and down (adapted from Koch & Yemshanov, 2015). As an example, for A_{p1i} in Eq. (2), the original "3 · weight" was replaced by 3.3, 3.6, 4.5, 2.7, 2.4 and 1.5, and on each occasion the number of census tracts that switched categories (from relatively low to high hazard levels, or vice versa, as defined in Section 2.4.5) was calculated. This was performed in turns, maintaining all the other parameters equal. Secondary factors were either omitted or their weights were duplicated, and once again the number of census tracts that switched categories was calculated. Regarding the vulnerability index, each primary factor was removed or duplicated in turns in Eq. (6). The R^2 coefficient of the linear regression between each modified vulnerability and the original vulnerability values per census tracts, along with the minimum, maximum and 1st and 3rd quartiles of the residuals of such regression were calculated.

3. Results

3.1. Hazard maps

The four hazard maps (based on air pollution, water pollution, and rodent and mosquito infestation indexes) show that hazard indexes are spatially heterogeneous over the study area (Fig. 3). Hazard values per census tract were positively and significantly autocorrelated ($p < 0.0001$; Moran's *I* index varying between 0.32 (air quality) and 0.83 (mosquito infestation)). However, not all the hazard indexes showed the same spatial pattern (Fig. 3), as can be noted in the spatial association between pairs of hazard maps (slopes of geographically weighted regressions; Fig. 4). In particular, air pollution was not significantly associated with the other hazard indexes ($p > 0.01$; and slopes close to 0 in most of the census tracts). The remaining hazard indexes were associated ($p < 0.0001$), with a varying slope along the census tracts. The highest spatial association was observed between mosquito and rodent hazards ($p < 0.0001$, $R^2 = 0.88$, median GWR slope 0.71, range 0.27–2.06; Fig. 4c). A North-South section covering several census tracts denotes a sector with similar (GWR slopes *ca.* 1) or relatively higher hazard for rodent than for mosquito infestation (GWR slopes >1; Fig. 4a). Since mosquito and rodent hazard maps were correlated, they showed a similar spatial association with water pollution hazard (Fig. 4a and b; $p < 0.0001$, $R^2 = 0.50$ for mosquitoes and 0.43 for rodents; median GWR slopes 0.14 and 0.12, respectively; range 0.01–0.95). Two hotspots where mosquito, rodent and water hazards were similar and relatively high were detected at the North-West and South-East zones of the study area (Fig. 4a and b, see also Fig. 3).

Threshold values for relatively low and high hazards were 0.38 for air pollution, 0.26 for mosquito infestation and 0.36 for rodent infestation. Water pollution index values presented a highly skewed distribution, therefore Jenks' Natural Break (threshold 0.22) classified only 3.2% of the census tracts as "high": we decided to adopt 0.01 as the threshold,

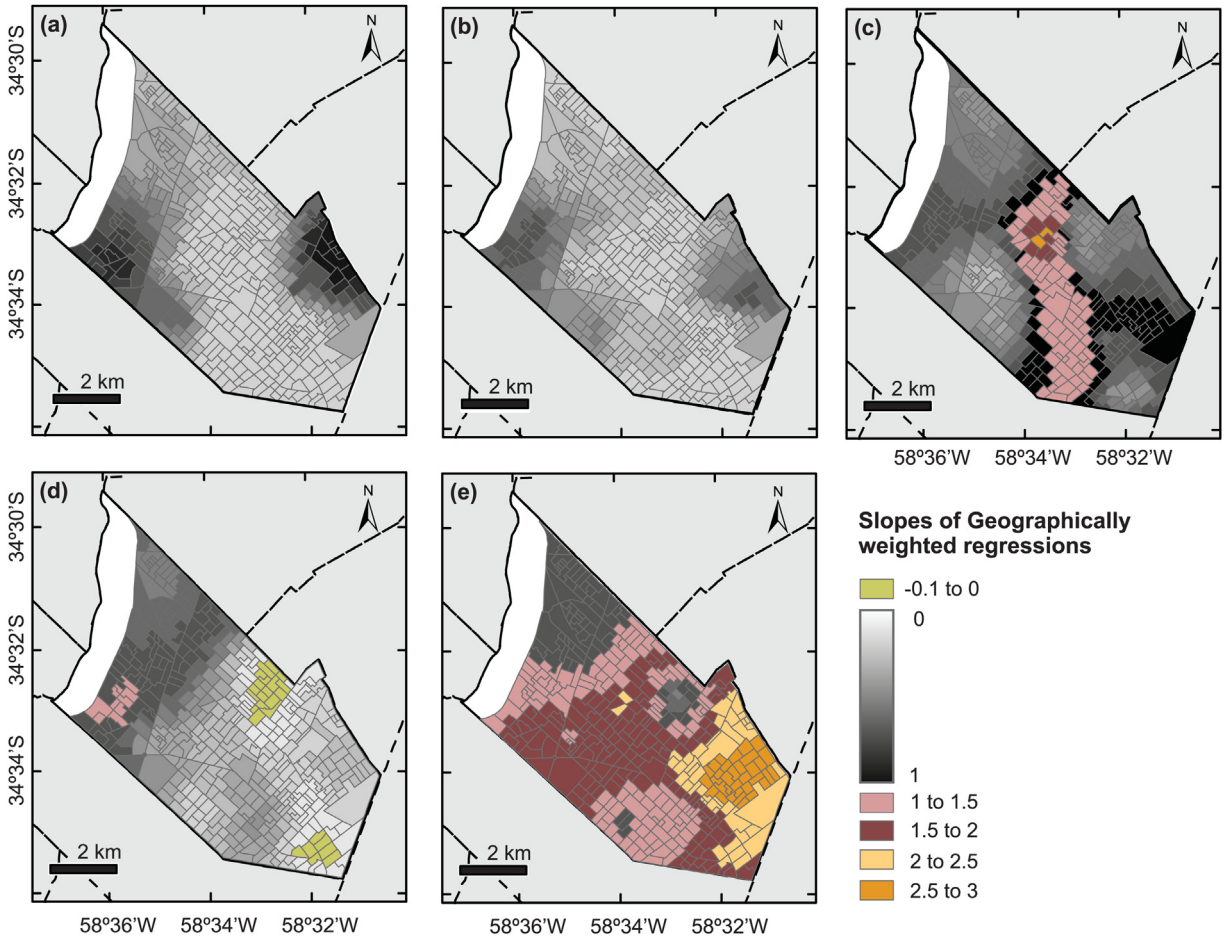

Fig. 4. Slopes of geographically weighted regressions per census tract. Significant regressions are shown. Greyscale was used for values between 0 and 1; and colors were used for values lower than 0 and higher than 1 (see electronic version for color images). Slopes correspond to the regression between: (a) Mosquito infestation hazard as a function of Water pollution hazard; (b) Rodent infestation hazard as a function of Water pollution hazard; (c) Rodent infestation hazard as a function of Mosquito infestation hazard; (d) Vulnerability index as a function of hazard intensity index; (e) Risk index as a function of hazard intensity index.

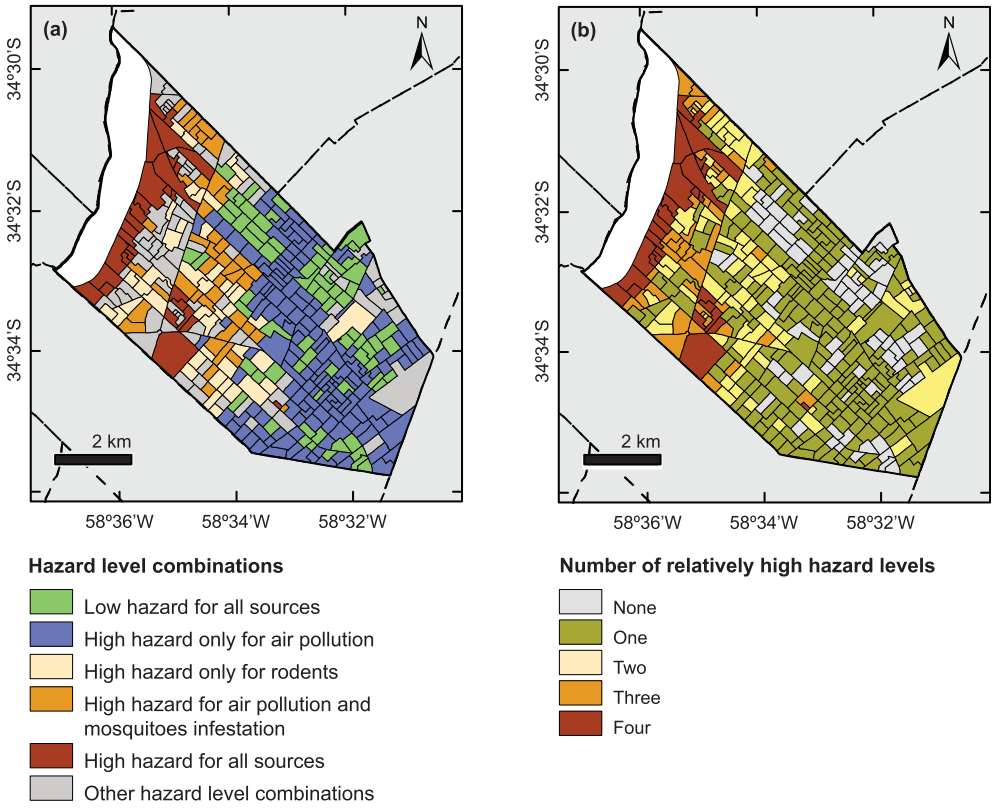

Fig. 5. Hazard types. (a) Hazard level combinations. (b) Number of relatively high hazard levels. See electronic version for color images.

which classified 21.9% of the census tracts as relatively high hazard level.

The combination of hazard levels was spatially structured, showing clusters of census tracts assigned to the same category (Fig. 5a). Low levels of all hazards were obtained in 16.6% of the census tracts (15.4% of the total area, 16.7% of the total population) (Table 2). High levels of all hazards occurred in 6.9% of the census tracts (11.5% of the total area, 7.4% of the total population). A high level of air pollution and a low level for the remaining sources was the most common combination, with 36.6% of the census tracts (31.2% of the total area and an exposed population of 31.8%). Most of the study area was exposed to relatively high levels of at least one hazard (Fig. 5b, Table 2): 83.5% of the census tracts, 84.7% of the total area and 83.3% of the population. Hazard intensity was spatially structured, showing autocorrelation ($p < 0.0001$, Moran's I index 0.71) (Fig. 6a).

Table 2
Census tracts, areas and exposed population in each category of hazard types. Results are summarized per relative hazard levels and per number of sources (water, air, mosquitoes or rodents) with relatively high hazard levels.

Hazard	Census tracts		Area		Exposed population*	
	Number	%	km^2	%	Inhabitants	%
Per hazard levels						
Low hazard for all sources	72	16.6	7.7	15.4	69,137	16.7
High hazard for air pollution	159	36.6	15.6	31.2	131,509	31.8
High hazard for rodents	44	10.1	6.1	12.1	50,206	12.1
High hazard due for air and mosquitoes	43	9.9	5.0	9.9	42,731	10.3
High hazard for all sources	30	6.9	5.8	11.5	30,493	7.4
Other hazard level combinations	86	19.9	10.0	19.9	89,816	21.7
Per number of sources with high hazard						
No high hazard levels	72	16.6	7.7	15.4	69,137	16.7
One high hazard levels	216	49.8	23.1	46.0	195,966	47.3
Two high hazard levels	74	17.1	9.3	18.5	76,929	18.6
Three high hazard levels	42	9.7	4.4	8.7	41,367	10
Four high hazard levels	30	6.8	5.8	11.4	30,493	7.4

* Total exposed population (413,982 inhabitants) is lower than the total General San Martín population (414,196 inhabitants); this is due to the exclusion of a census tract outside the study area and with 304 inhabitants (0.07% of the population).

3.2. Vulnerability and risk maps

Both vulnerability and risk maps showed spatial autocorrelation ($p < 0.0001$, Moran's *I* index 0.61 and 0.68, respectively; Fig. 6b and c). The vulnerability map was spatially correlated to the hazard intensity map ($p < 0.0001$, $R^2 = 0.67$, median GWR slope 0.27, range -0.09–1.07; Fig. 4d); and the risk map was spatially correlated to the hazard map ($p < 0.0001$, $R^2 = 0.84$, median GWR slope 1.54, range 0.53–3.04; Fig. 4e). In other words, those areas where hazard intensity was relatively high were coincident with areas where the most vulnerable population live, leading to a higher risk to human health. In particular, a hotspot with high and similar hazard and vulnerability index values occurred in the North-West section of the study area (Fig. 6).

3.3. Sensitivity analysis

Very stable results were obtained for two of the hazard indexes. For rodent infestation, all changes in the weights assigned to hazard indexes resulted in less than 2% of the census tracts switching categories. For water pollution, all weight changes affected <10% of the census tracts, and the source of water used for human consumption W_{s1} was the most affecting variable. Regarding mosquito infestation, all changes resulted in <7% of census tracts switching categories, except when we considered a reduction of 50% in the weight affecting the percentage of households without a sewer connection (*Mp4*). This resulted in 92 out of the 434

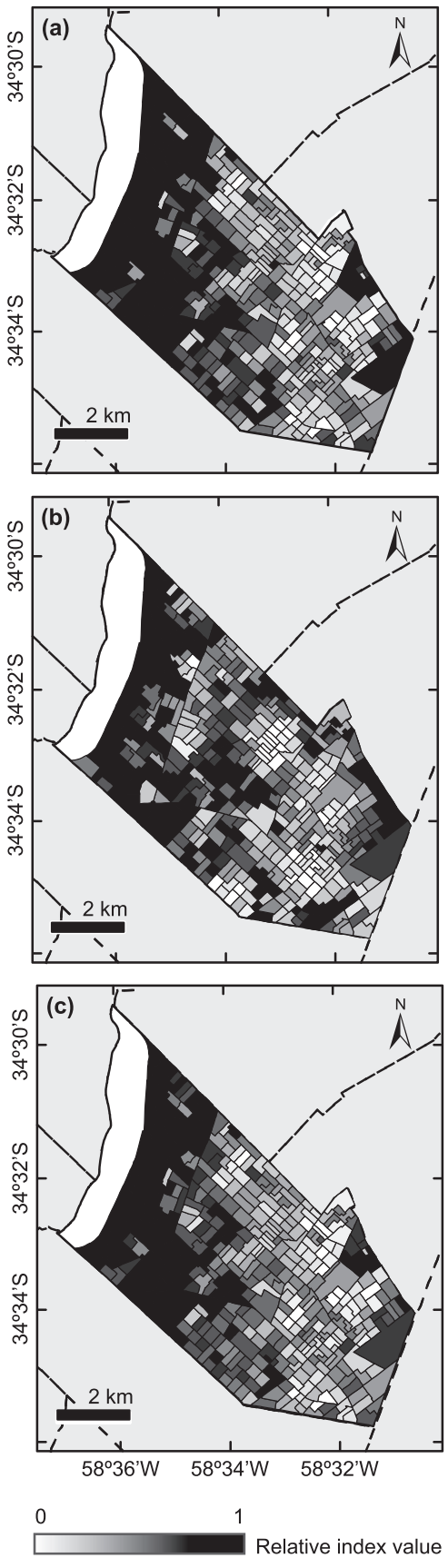

Fig. 6. Product maps. (a) Hazard intensity map. (b) Vulnerability map. (c) Risk map.

census tracts (21.2%) of the tracts changing from relatively high to low hazard levels. Lastly, when analyzing the air pollution map, all changes resulted in <13% of the census tracts switching categories except in two cases. When increasing the weight assigned to the proximity to gas stations (A_{p1}) by 50%, 77 out of the 434 census tracts (17.7%) switched categories, mainly from relatively high to low hazard levels. When reducing the weight assigned to vehicular and train emissions (A_{p2}) by 50%, 121 out of the 434 census tracts (27.9%) switched categories. Remarkably, when increasing the weight of A_{p2} by 50% no significant change was observed, probably because the hazard index increased further (from relatively high to a non-discriminated very high category).

Modified vulnerability index values per census tract as a result of removing or duplicating each primary factor were highly correlated with the original values (R^2 coefficients in the range 0.89–0.99, Table 3). The lowest correlation coefficient was obtained by removing the Distance to primary health centers (V_6), in which a maximum change in 0.24 in the vulnerability index value was recorded and the 1st quartile of the values was modified in -0.07. All other changes resulted in modified vulnerability index values within -0.03 and 0.03 for 1st and 3rd quartiles (Table 3), showing high robustness.

4. Discussion

This interdisciplinary approach contributes to the territorial representation of environmental hazards, social vulnerability and the resulting risk to human health in a complex urban environment. Georeferenced data are integrated into a GIS framework by means of statistical tools and with an urban landscape ecology approach. Our study constitutes an unprecedented baseline for General San Martín, Argentina. The methodology allows for the spatial representation at a district scale of the risk derived from one or more hazards, and can be thought as a modular, dynamic and perfectible scheme as more studies are performed in the area and novel information regarding these or other hazards becomes available. The expected outputs (hazard, vulnerability and risk indexes) can be a valuable tool for policy-makers; as well as a baseline to plan environmental measurements and to monitor environmental and human health indicators.

General San Martín has been pointed out as the third riskiest district of Argentina in terms of child health mainly due to high levels of industrial pollution and social vulnerability (Maiztegui and Delucchi, 2010), and is among the four districts of Buenos Aires Province with more environmental problems (Velázquez and Celemín, 2013). Our hazard maps reinforce this alarming situation since over 83% of the population is exposed to relatively high levels of at least one of the considered hazards, and almost 7% is exposed to relatively high levels of the four hazards. In a previous study in this district, variables related to vulnerability have been analyzed within a sociological framework using GIS tools (Álvarez and Iulita, 2006). However, this is the first study addressing the spatial patterns of environmental hazards and risks.

Spatial heterogeneity needs to be addressed in environmental management policies: our results showed that the studied hazard sources (air pollution, water pollution, and rodent and mosquito infestation) are not homogeneously distributed along the study area. With the exception of air pollution, hazards were positively spatially autocorrelated and high levels were clustered in the North-West (NW) section of the study area, particularly in two hotspots. This denotes the need to guarantee basic sanitary conditions and thus prioritize access to safe drinking water, garbage disposal, mosquito and rodent control, and development of green spaces, among other issues, in these hotspots. Unfortunately, areas with higher hazard levels coincide with those of greatest vulnerability. The population in the NW area of the district has fewer tools to avoid or mitigate the impact of any threat to their health. Therefore, prevention and control of environmental hazards must be coupled with improving access to health care and education (Kjellstrom et al., 2007).

The greatest geographic associations were found between biological hazards (mosquito and rodent infestation), as expected since some of the

Table 3
Sensitivity analyses for the vulnerability index. In turns, each of the variables included in the vulnerability index (V_1 to V_6) was removed or its weight was duplicated. The modified index was regressed onto the original one: R^2 adjust and descriptors of the residuals are summarized.

Variable	Action	R^2	Residuals			
			Minimum	1st quartile	3rd quartile	Maximum
V_1. Proportion of children and elderly population	Remove	0.956	-0.15	-0.02	0.02	0.10
	Duplicate	0.975	-0.07	-0.01	0.01	0.11
V_2. Overcrowding	Remove	0.967	-0.13	-0.01	0.02	0.07
	Duplicate	0.986	-0.04	-0.01	0.01	0.08
V_3. Illiteracy rate	Remove	0.965	-0.21	-0.01	0.02	0.10
	Duplicate	0.983	-0.06	-0.01	0.01	0.13
V_4. Economic inactivity	Remove	0.937	-0.16	-0.02	0.02	0.11
	Duplicate	0.961	-0.09	-0.02	0.02	0.12
V_5. Poor quality of construction materials	Remove	0.911	-0.13	-0.03	0.03	0.13
	Duplicate	0.983	-0.07	-0.01	0.01	0.07
V_6. Distance to primary health centers	Remove	0.887	-0.17	-0.07	0.01	0.24
	Duplicate	0.911	-0.09	-0.03	0.03	0.14

primary factors were shared by these hazard indexes. While water pollution hazard hotspots were partially coincident with the NW area, air pollution hazard showed a contrasting spatial pattern. Air pollution depends on emission sources that are not only restricted to the NW area with the highest social vulnerability (Fig. 6c), such as industries and vehicular traffic. The effect of industries on environmental hazards and risk was expected: General San Martín is one of the districts with the highest industrial development in Buenos Aires Province (Fritzsche and Vio, 2000).

The spatial patterns of environmental hazards here reported are an emergent landscape feature of environmental problems associated with unplanned urbanization. Two main urbanization processes can be recognized in the district (Álvarez, 2005; Chiaramonte, 2005; Paredes, 2010): settlements close to industries during a stage of industrial development (beginning in the 1930s, important during the 1940s–50s); and settlements in low topography areas, beginning in the 1970s–1980s, close to Reconquista River (NW area of the district), and nowadays exposed to flooding and close to dumps and landfills. We suggest that the distinct spatial pattern observed for the air pollution hazard map is the combined product of potential air pollution related to industrial activities and to high-vehicular traffic zones associated to the proximity of Buenos Aires city and to the main vehicular access, including trucks and urban transport; superimposed to hazard zones related to the NW area close to dump and landfills. On the other hand, the other hazard sources would mainly reflect the second unplanned urbanization process. Thus, several historical processes of unplanned urbanization would be potentially interacting to generate the environmental hazard patterns at a landscape scale.

Our results support social and infrastructure asymmetries previously reported for urban districts close to the Argentinean capital city: highly populated low-income settlements or slums in areas with limited access to safe drinking water, inexistent sewer connection and insufficient garbage disposal, access to public health services and education, among other issues (Curutchet et al., 2012; Paredes, 2010; Velázquez and Celemín, 2013). Such spatial heterogeneity has been observed in other urban areas (*e.g.,* Kaźmierczak and Cavan, 2011). The methodological proposal presented herein can be replicated in other temperate urban areas, adapting the conceptual framework to any other environmental hazards using the same (or other) data sources and weighting criteria. It is worth mentioning that low and high risk categories are comparative solely within the district they were developed, as no theoretical criterion for low and high levels was taken for each hazard, rather a replicable standardized procedure using Jenks' breaks was preferred. Even though this methodology does not allow for the estimation of absolute risk values, the detection of areas with relatively high risk values is necessary to focusing and optimizing the implementation of environmental sanitation and the reduction of levels of social vulnerability (Di Salvo et al., 2018).

Addressing uncertainties in human health risk assessment is important for effective decision making, highlighting the implications and limitations of the obtained models. The lack of robustness is one of the contributors to uncertainties and can be assessed through sensitivity analyses (Arunraj et al., 2013; Dong et al., 2015). According to our results, the models for each hazard and vulnerability were robust to changes in the weights given to the variables considered. In the few cases in which this did not hold and many census tracts switched categories, they did so mainly from relatively high to low hazard levels: *i.e.*, a conservative situation in which hazard would be ultimately overestimated. This is preferred over underestimation in terms of protection of the population, but would lead to squandered resources. Having identified the critical variables, *i.e.,* those with a greater effect on the uncertainty of hazard estimations, future research can be focused on improving their measure and the estimation of their weights (Barrio-Parra et al., 2019). Regarding air pollution, a reduction in the weight of vehicular and train emissions by 50% was the only case (out of 28 different combinations of parameters tested) in which the hazard index was not robust. This index may be improved by including more reliable data on annual average daily traffic, rather than assuming high traffic where public transport circulation occurs. Unfortunately, such records are still unavailable. Besides, the sensitivity analysis allowed for the identification of some secondary factors that did not have a significant effect on the hazard outcome. Such variables, that may be unavailable or measured with a high level of uncertainty in other areas, could be omitted in future analyses.

At the district scale, our map distinguished the most relevant areas for human health from an environmental point of view, considering the census tract as the minimal sampling unit. The criterion for this selection was related to the minimum unit for which information was available with the required degree of detail. Hazard and risk analyses can also be conducted at a more detailed scale, such as a neighborhood, or also at a regional or country scale. Other variables might then be appropriate since their effect on hazard, vulnerability and risk indexes may be scale-dependent (McGranahan et al., 2001) and vary when disaggregating data (Maantay and Maroko, 2009). Regarding the temporal scale, our approach characterized the current state of hazards, vulnerability and risk in a static snapshot corresponding mainly to the last decade, due to the inclusion of data from the last National Census of Population conducted in 2010 (Instituto Nacional de Estadística y Censos, 2010). Long-term temporal studies of risk change would be desirable (Bień et al., 2005), to assess the effect of urban growth and the impact of possible improvements in access to public services, environmental management and sanitation.

The hazards considered in this study (*i.e.*, water and air pollution, mosquito and rodent infestation) affect human health in a wide range of urban areas (McGranahan et al., 2001; Moore et al., 2003), but other hazards related to inherent features of the urban living environment (*e.g.*

building conditions, energy and food demands, climate change) could be easily added to the methodological scheme (Kjellstrom et al., 2007). Some examples are flood hazard and electric hazard due to poor wiring and precarious connections to energy (increasing the probability of fires and electrocution) (Ahmed, 2016). Likewise, vulnerability estimations could be optimized by the inclusion of variables that consider social, economic and environmental aspects related to local sanitary problems (Kaźmierczak and Cavan, 2011). The estimation of environmental hazards and sanitary risk is substantially improved if immersed in an interdisciplinary urban ecological view linked with a sociological approach, addressing the social perception of risks and the participation of community organizations (Merlinsky, 2013).

5. Conclusion

Risk is heterogeneous and multidimensional. The development of tools to measure and assess risk exposure, and to organize mitigation and reduction actions are configured as essential ingredients of any management strategy. Our contribution is to provide a methodological framework to analyze environmental hazards, vulnerability and risks, and to assess their spatial relations. We consider that our conceptual framework is valuable because it integrates theories and tools from urban and landscape ecology, spatial statistics and GIS approaches. For policy-makers, risk assessments need to be informed or summarized in technical (non-academic) language, in a clear and simple manner, and in the native language of the local population (in our case study, Spanish). In this way, the local population and decision-makers can discuss policies and participate in prevention and mitigation actions. Notwithstanding, these sources of sanitary risk are beyond the exclusive control of individuals, as they require the action of decision-makers and a firm regulation background. Therefore, management organisms and local politicians need baseline studies, to which we intend to contribute. A risk map of this nature provides georeferenced and integrated information about hazard, vulnerability and risks.

This study generated hypotheses on the spatial arrangement of the territory regarding environmental hazards and risks to human health. Future work will include the assessment of these environmental hazards by field measures of air and water quality and the abundance of mosquitoes and rodents. The obtained hazard and risk maps will be an input for planning environmental health assessments, aiding in the design of sampling campaigns. The field validation of the risk map presented in this work will be critical to demonstrating that the considerations made for its elaboration were correct and will allow its use as a monitoring tool. With regard to possible inputs for policy-makers, we have already presented several technical reports to government agencies and neighborhood leaders.

Declarations

Author contribution statement

Natalia Soledad Morandeira, Paula Soledad Castesana, María Victoria Cardo, Vanesa N. Salomone, María Victoria Vadell, Alejandra Rubio: Conceived and designed the experiments; Performed the experiments; Analyzed and interpreted the data; Contributed reagents, materials, analysis tools or data; Wrote the paper.

Funding statement

The study was funded by the Instituto de Investigaciones e Ingeniería Ambiental, Universidad Nacional de San Martín (3iA - UNSAM, Argentina).

Competing interest statement

The authors declare no conflict of interest.

Additional information

No additional information is available for this paper.

Acknowledgements

We wish to thank Anibal Carbajo for his contributions to the regionalization procedure; and to Regino Cavia and two anonymous reviewers for their valuable comments and suggestions. Laura San Martín and Véronique Pestoni helped with the design of the graphical abstract. WorldView-3 imagery is courtesy of the DigitalGlobe Foundation. We also thank all the organizations and individuals that provided information and spatial layers: Secretaría de Extensión Universitaria (UNSAM), through their Territorial Information System; Secretaría de Energía de la Nación, through their Geographic Information System; Organismo Provincial para el Desarrollo Sustentable (OPDS), through their Direction of Evaluation of Environmental Impact; Alejandro Cittadino and Alicia Álvarez (CEAMSE); Mariela Miño; Ariel Werner (Universidad Tecnológica Nacional).

References

Ahmed, I., 2016. Building resilience of urban slums in Dhaka, Bangladesh. Procedia-Soc. Behav. Sci. 218, 202–213.

Álvarez, G.H., 2005. Gran Buenos Aires, conurbano y Partido de San Martín: exclusión social y segregación urbana. Scr. Nov. IX, 1–24.

Álvarez, G.H., Iulita, A., 2006. SIG aplicado a la detección de áreas de riesgo y vulnerabilidad social en el Partido de San Martín, Buenos Aires, Argentina. In: Erba, D.A. (Ed.), Sistemas de Información Geográfica Aplicados a Estudios Urbanos. Experiencias Latinoamericanas. Lincoln Institute of Land Policy, Massachusetts, USA, pp. 165–176.

Arunraj, N.S., Mandal, S., Maiti, J., 2013. Modeling uncertainty in risk assessment: an integrated approach with fuzzy set theory and Monte Carlo simulation. Accid. Anal. Prev. 55, 242–255.

Barrio-Parra, F., Izquierdo-Díaz, M., Dominguez-Castillo, A., Medina, R., De Miguel, E., 2019. Human-health probabilistic risk assessment: the role of exposure factors in an urban garden scenario. Landsc. Urban Plan. 185, 191–199.

Bień, J.D., ter Meer, J., Rulkens, W.H., Rijnaarts, H.H.M., 2005. A GIS-based approach for the long-term prediction of human health risks at contaminated sites. Environ. Model. Assess. 9, 221–226.

Bivand, R.S., Keitt, T., Rowlingson, B., 2018. Rgdal: Bindings for the Geospatial Data. Abstraction Library.

Bivand, R.S., Pebesma, E.J., Gómez-Rubio, V., 2008. Applied Spatial Data Analysis with R. Springer, New York, US.

Bivand, R.S., Piras, G., 2015. Comparing implementations of estimation methods for spatial econometrics. J. Stat. Softw. 63, 1–36.

Brito, E.M., Cruz Barrón, M., Caretta, C., Goñi-Urriza, M., Andrade, L., Cuevas-Rodríguez, G., Malm, O., Torres, J., Simon, M., Guyoneaud, R., 2015. Impact of hydrocarbons, PCBs and heavy metals on bacterial communities in Lerma River, Salamanca, Mexico: investigation of hydrocarbon degradation potential. Sci. Total Environ. 521, 1–10.

Brooks, N., 2003. Vulnerability, risk and adaptation: a conceptual framework. Tyndall Cent. Clim. Chang. Res. Work. Pap. 38, 1–16.

Cabral, J., 2010. Water microbiology. Bacterial pathogens and water. Int. J. Environ. Res. Public Health 7, 3657–3703.

Carvalho de Oliveira, R., Guterres, A., Fernandes, J., D'Andrea, P., Bonvicino, C., de Lemos, E., 2014. Hantavirus reservoirs: current status with an emphasis on data from Brazil. Viruses 6, 1929–1973.

Cavia, R., Cueto, G.R., Suárez, O.V., 2009. Changes in rodent communities according to the landscape structure in an urban ecosystem. Landsc. Urban Plan. 90, 11–19.

Chiaramonte, M., 2005. El sector de pequeñas y medianas industrias del Partido de San Martín frente al proceso de desindustrialización: 1990-2002. Doc. Trab. la Esc. Política y Gob UNSAM 11, 1–28.

Correa, S., Arbilla, G., Marques, M., Oliveira, K., 2012. The impact of BTEX emissions from gas stations into the atmosphere. Atmos. Pollut. Res. 3, 163–169.

Curutchet, G., Grinberg, S., Gutiérrez, R.A., 2012. Degradación ambiental y periferia urbana: un estudio transdiciplinario sobre la contaminación en la región metropolitana de Buenos Aires. Ambient. Soc. 15, 173–194.

Di Salvo, C., Pennica, F., Ciotoli, G., Cavinato, G.P., 2018. A GIS-based procedure for preliminary mapping of pluvial flood risk at metropolitan scale. Environ. Model. Softw 107, 64–84.

Dong, Z., Liu, Y., Duan, L., Bekele, D., Naidu, R., 2015. Uncertainties in human health risk assessment of environmental contaminants: a review and perspective. Environ. Int. 85, 120–132.

Feng, A.Y., Himsworth, C.G., 2014. The secret life of the city rat: A review of the ecology of urban Norway and black rats *(Rattus norvegicus and Rattus rattus)*. Urban Ecosyst. 17, 149–162.

Fritzsche, F.J., Vio, M., 2000. Especialización y diversificación industrial en la Región Metropolitana de Buenos Aires. Eure 26, 25–45.

Gollini, I., Lu, B., Charlton, M., Brunsdon, C., Harris, P., 2015. {GWmodel}: an {R} package for exploring spatial heterogeneity using geographically weighted models. J. Stat. Softw. 63, 1–50.
Hagenlocher, M., Renaud, F.G., Haas, S., Sebesvari, Z., 2018. Vulnerability and risk of deltaic social-ecological systems exposed to multiple hazards. Sci. Total Environ. 631, 71–80.
Himsworth, C.G., Parsons, K.L., Jardine, C., Patrick, D.M., 2013. Rats, cities, people, and pathogens: a systematic review and narrative synthesis of literature regarding the ecology of rat-associated zoonoses in urban centers. Vector Borne Zoonotic Dis. 13, 349–359.
Hrudey, S.E., Hrudey, E.J., Pollard, S.J.T., 2006. Risk management for assuring safe drinking water. Environ. Int. 32, 948–957.
Hubbell, B., Hallberg, A., McCubbin, D., Post, E., 2005. Health-related benefits of attaining the 8-hr ozone standard. Environ. Health Perspect. 113, 73.
IARC Working Group, 2018. Benzene. IARC Monographs on the Evaluation of Carcinogenic Risks to Humans, vol. 120. International Agency for Research on Cancer, World Health Organization, Lyon, France.
Igarzabal de Nistal, M.A., Cittadino, A., Zamorano, J.A., Ocello, N., Majul, M.V., D'hers, V., Ajhuacho, R., 2012. Atlas de la Basura. Wolkowicz Editores, Buenos Aires, Argentina.
Instituto Nacional de Estadística y Censos, 2010. Censo nacional de población, hogares y viviendas 2010: censo del Bicentenario.
Irwin, P., Arcari, C., Hausbeck, J., Paskewitz, S., 2008. Urban wet environment as mosquito habitat in the Upper Midwest. EcoHealth 5, 49.
Jenks, G.F., Coulson, R.C., 1963. Class intervals for statistical maps. Int. Yearb. Cartogr. 119–134.
Jiang, L., O'Neill, B., 2017. Global urbanization projections for the shared socioeconomic pathways. Glob. Environ. Chang. 42, 193–199.
Kaźmierczak, A., Cavan, G., 2011. Surface water flooding risk to urban communities: analysis of vulnerability, hazard and exposure. Landsc. Urban Plan. 103, 185–197.
Kjellstrom, T., Friel, S., Dixon, J., Corvalan, C., Rehfuess, E., Campbell-Lendrum, D., Gore, F., Bartram, J., 2007. Urban environmental health hazards and health equity. J. Urban Health 84, 86–97.
Koch, F.H., Yemshanov, D., 2015. Identifying and assessing critical uncertainty thresholds in a forest pest risk model. In: Venette, R.C. (Ed.), Pest Risk Modelling and Mapping for Invasive Alien Species. CABI Publishing, Wallingford, UK, pp. 189–205.
Kubal, C., Haase, D., Meyer, V., Scheuer, S., 2009. Integrated urban flood risk assessment–adapting a multicriteria approach to a city. Nat. Hazards Earth Syst. Sci. 9, 1881–1895.
Lahr, J., Kooistra, L., 2010. Environmental risk mapping of pollutants: state of the art and communication aspects. Sci. Total Environ. 408, 3899–3907.
Lambert, M., Vial, F., Pietravalle, S., Cowan, D., 2017. Results of a 15-year systematic survey of commensal rodents in English dwellings. Sci. Rep. 7, 15882.
Lindley, S.J., Handley, J.F., Theuray, N., Peet, E., Mcevoy, D., 2006. Adaptation strategies for climate change in the urban environment: assessing climate change related risk in UK urban areas. J. Risk Res. 9, 543–568.
Liu, C., Wu, X., Wang, L., 2019. Analysis on land ecological security change and affect factors using RS and GWR in the Danjiangkou Reservoir area, China. Appl. Geogr. 105, 1–14.
Maantay, J., Maroko, A., 2009. Mapping urban risk: flood hazards, race, & environmental justice in New York. Appl. Geogr. 29, 111–124.
Maiztegui, C., Delucchi, M., 2010. Niñez y Riesgo Ambiental en Argentina. Defensor del Pueblo de la Nación; PNUD Argentina; Unicef Argentina; Organización Panamericana de la Salud; Oficina Internacional del Trabajo.
Majumdar, D., Ray, S., Chakraborty, S., Rao, P., Akolkar, A., Chowdhury, M., Srivastava, A., 2014. Emission, speciation, and evaluation of impacts of non-methane volatile organic compounds from open dump site. J. Air Waste Manag. Assoc. 64, 834–845.
Marzocchi, W., Garcia-Aristizabal, A., Gasparini, P., Mastellone, M.L., Di Ruocco, A., 2012. Basic principles of multi-risk assessment: a case study in Italy. Nat. Hazards 62, 551–573.
Masi, E., Pino, F.A., das Graças, S.S., Genehr, L., Albuquerque, J.O.M., Bancher, A.M., Alves, J.C.M., 2010. Socioeconomic and environmental risk factors for urban rodent infestation in Sao Paulo, Brazil. J. Pest. Sci. 83, 231–241, 2004.
McGranahan, G., Jacobi, P., Songsore, J., Surjadi, C., Kjellén, M., 2001. The Citizens at Risk: from Urban Sanitation to Sustainable Cities. Earthscan, London, UK.
Meerburg, B.G., Singleton, G.R., Kijlstra, A., 2009. Rodent-borne diseases and their risks for public health. Crit. Rev. Microbiol. 35, 221–270.
Merlinsky, M.G., 2013. Cartografías del conflicto ambiental en Argentina. Ediciones CICCUS.
Miño, M.L., 2012. Detección de basurales ilegales, rellenos sanitarios, ex basurales, tosqueras y chatarreras en el Gran Buenos Aires, mediante teledetección y sistemas de información geográfica. Instituto Gulich, Universidad Nacional de Córdoba.
Moore, M., Gould, P., Keary, B., 2003. Global urbanization and impact on health. Int. J. Hyg Environ. Health 206, 269–278.
Paciência, I., Madureira, J., Rufo, J., Moreira, A., Fernandes de Oliveira, E., 2016. A systematic review of evidence and implications of spatial and seasonal variations of volatile organic compounds (VOC) in indoor human environments. J. Toxicol. Environ. Health Part B 19, 47–64.
Paredes, L., 2010. Fragmentación socioespacial y oferta educativa de nivel secundario en el Partido de General San Martín, Provincia de Buenos Aires. In: VI Jornadas de Sociología de La UNLP, pp. 1–20.
Poggio, L., Vrščaj, B., 2009. A GIS-based human health risk assessment for urban green space planning-An example from Grugliasco (Italy). Sci. Total Environ. 407, 5961–5970.
R Core Team, 2015. R: A Language and Environment for Statistical Computing.
Rabosky, D.L., Grundler, M.C., Anderson, C.J., Title, P.O., Shi, J.J., Brown, J.W., Huang, H., Larson, J.G., 2014. BAMMtools: an R package for the analysis of evolutionary dynamics on phylogenetic trees. Method. Ecol. Evol. 5, 701–707.
Rubio, A., Cardo, M.V., Carbajo, A.E., Vezzani, D., 2013. Imperviousness as a predictor for infestation levels of container-breeding mosquitoes in a focus of dengue and Saint Louis encephalitis in Argentina. Acta Trop. 128, 680–685.
Schmidt, W.-P., Suzuki, M., Thiem, V.D., White, R.G., Tsuzuki, A., Yoshida, L.-M., Yanai, H., Haque, U., Anh, D.D., Ariyoshi, K., 2011. Population density, water supply, and the risk of dengue fever in Vietnam: cohort study and spatial analysis. PLoS Med. 8, e1001082.
Singleton, G.R., Hinds, L.A., Krebs, C.J., Spratt, D.M., 2003. Rats, Mice and People: Rodent Biology and Management.
Tamayo-Uria, I., Mateu, J., Escobar, F., Mughini-Gras, L., 2014. Risk factors and spatial distribution of urban rat infestations. J. Pest Sci. 87, 107–115.
Taylor, R., Allen, A., 2006. Waste disposal and landfill: potential hazards and information needs. In: Schmoll, O., Howard, G., Chilton, J., Chorus, I. (Eds.), Protecting Groundwater for Health: Managing the Quality of Drinking-Water Sources. World Health Organization, London, UK, pp. 339–362.
Traweger, D., Travnitzky, R., Moser, C., Walzer, C., Bernatzky, G., 2006. Habitat preferences and distribution of the brown rat (*Rattus norvegicus* Berk.) in the city of Salzburg (Austria): implications for an urban rat management. J. Pest. Sci. 79, 113–125, 2004.
Tucker, C.J., 1979. Red and photographic infrared linear combinations for monitoring vegetation. Remote Sens. Environ. 150, 127–150.
Velázquez, G.Á., Celemín, J.P., 2013. La calidad ambiental en Argentina. Análisis regional y departamental (c.2010). Universidad Nacional del Centro de la Provincia de Buenos Aires, Buenos Aires, Argentina.
Verdonschot, P.F.M., Besse-Lototskaya, A.A., 2014. Flight distance of mosquitoes (Culicidae): a metadata analysis to support the management of barrier zones around rewetted and newly constructed wetlands. Limnol. Manag. Inl. Water. 45, 69–79.
Vezzani, D., 2007. Review: artificial container-breeding mosquitoes and cemeteries: a perfect match. Trop. Med. Int. Health 12, 299–313.
vonHedemann, N., Butterworth, M.K., Robbins, P., Landau, K., Morin, C.W., 2015. Visualizations of mosquito risk: a political ecology approach to understanding the territorialization of hazard control. Landsc. Urban Plan. 142, 159–169.
Weaver, S.C., Charlier, C., Vasilakis, N., Lecuit, M., 2018. Zika, Chikungunya, and other emerging vector-borne viral diseases. Annu. Rev. Med. 69, 395–408.
World Health Organization, 2016. Ambient Air Pollution: a Global Assessment of Exposure and burden of Disease. World Health Organization, Geneva, Switzerland.
World Health Organization, 2014. A Global Brief on Vector-Borne Diseases. World Health Organization.
World Health Organization, 2011. Guidelines for Drinking-Water Quality, Fourth. ed. World Health Organization, Geneva, Switzerland.